

DEUTSCHES ELEKTRONEN-SYNCHROTRON  
in der HELMHOLTZ-GEMEINSCHAFT



DESY 02-151  
September 2002

## Uncertainties in Track Momentum due to Multiple Scattering in a Forward Spectrometer

A. Spiridonov

*Deutsches Elektronen-Synchrotron DESY, Zeuthen*



ISSN 0418-9833

PLATANENALLEE 6 - 15738 ZEUTHEN

DESY behält sich alle Rechte für den Fall der Schutzrechtserteilung und für die wirtschaftliche Verwertung der in diesem Bericht enthaltenen Informationen vor.

DESY reserves all rights for commercial use of information included in this report, especially in case of filing application for or grant of patents.

To be sure that your reports and preprints are promptly included in the  
HEP literature database  
send them to (if possible by air mail):

DESY  
Zentralbibliothek  
Notkestraße 85  
22603 Hamburg  
Germany

DESY  
Bibliothek  
Platanenallee 6  
15738 Zeuthen  
Germany

# Uncertainties in Track Momentum due to Multiple Scattering in a Forward Spectrometer

Alexander Spiridonov\*  
DESY Zeuthen

September 24, 2002

## Abstract

The influence of multiple scattering on the momentum resolution for a forward spectrometer is investigated. Two cases, with and without track measurements inside the magnet, are discussed. A simple relation between angular and momentum resolutions and multiple scattering inside the magnet is derived and confirmed with Monte Carlo generated events subjected to a detailed simulation and full reconstruction for a real spectrometer.

## 1 Introduction

Experiments dedicated to the study of heavy flavour production in hadron-nucleon collisions are designed as forward spectrometers because the decay particles of the heavy flavours are produced with a large Lorentz boost. The tracking system of a forward spectrometer includes at least two parts: tracking detectors in front of the magnet and behind it. If a considerable fraction of interesting decays are too late to be measured in front of the magnet, then additional tracking detectors placed inside the magnet are useful. Spectra of particles are almost exponentially depending on momentum and the effect of multiple scattering is important for the majority of reconstructed tracks even for a high energy primary collision.

In Section 2 we will consider the limitations for the track parameter resolution in a forward spectrometer using the Cramèr-Rao inequality. In Sections 3 and 4 models of a spectrometer with and without track measurement inside the magnet will be discussed and simple relations for resolutions will be derived. The obtained relations will be tested with the simulation of the HERA-B spectrometer [1] presenting an example of a modern detector with a sufficiently complicated structure and an inhomogeneous magnetic field. The detector, Monte Carlo simulation and reconstruction will be described in Section 5. In Section 6, relations describing the influence of multiple scattering on momentum resolution will be compared with the results of detailed simulations and the actual reconstruction procedure.

## 2 Momentum resolution and multiple scattering

Let us consider a forward spectrometer as a set of detector planes where track parameters are measured. The index  $i$  of a detector plane runs from 1 up to  $N$ . The  $z$  axis of the coordinate system points along the primary beam, the  $x$  axis belongs to the bending plane of the magnet and the  $y$  axis is oriented parallel to the main component of the magnetic field. The measurement of a track in one plane is  $U_i$ , one of  $N$  components of the measurement vector  $\mathbf{U}$ . For the moment, we do not specify a model of measurement.

The vector  $\mathbf{v}$  defines track parameters in the position of the first plane ( $i = 1$ ). A typical parameter set for fixed target experiments with relatively small transverse momenta with respect to the longitudinal axis for a particle with momentum  $\vec{p}$ , charge  $Q$  and coordinate  $\vec{x}$  is described by the vector

$$\mathbf{v}^T = (x, y, t_x, t_y, q),$$

where  $x$  and  $y$  are the transverse coordinates,  $t_x = p_x/p_z$  and  $t_y = p_y/p_z$  are the track slopes, and  $q = Q/|\vec{p}|$  is used as momentum parameter at the  $z$  value of reference. Usually the slopes  $t_x$  and  $t_y$  are small.

The conditional probability density of a vector  $\mathbf{U}$  for given initial track parameters  $\mathbf{v}$

---

\*Permanent address: Institute of Theoretical and Experimental Physics, 117259 Moscow, Russia

is described by the expression

$$f(\mathbf{U} | \mathbf{v}) = (2\pi)^{-\frac{N}{2}} |\mathbf{C}_{\mathbf{U}}|^{-\frac{1}{2}} \exp\left[-\frac{1}{2}(\mathbf{U} - \mathbf{E}(\mathbf{U}))^T \mathbf{C}_{\mathbf{U}}^{-1} (\mathbf{U} - \mathbf{E}(\mathbf{U}))\right], \quad (1)$$

where  $|\mathbf{C}_{\mathbf{U}}|$  is the determinant of the covariance matrix  $\mathbf{C}_{\mathbf{U}}$  of the vector  $\mathbf{U}$  and

$$\mathbf{E}(\mathbf{U}) = \bar{\mathbf{U}}(\mathbf{v})$$

is its mean value. Both the matrix  $\mathbf{C}_{\mathbf{U}}$  and the vector  $\bar{\mathbf{U}}(\mathbf{v})$  are functions of the track parameters  $\mathbf{v}$ .

The Cramér–Rao inequality [2] defines a lower bound for the covariance matrix  $\mathbf{C}_{\hat{\mathbf{v}}}$  of the parameters estimate  $\hat{\mathbf{v}}$

$$\mathbf{C}_{\hat{\mathbf{v}}} \geq \mathbf{I}^{-1}, \quad (2)$$

where  $\mathbf{I}$  is the information matrix

$$I_{ij} = \mathbf{E} \left( -\frac{\partial^2 \ln f(\mathbf{U} | \mathbf{v})}{\partial v_i \partial v_j} \right). \quad (3)$$

The inequality 2 means that a quadratic form involving any vector  $\mathbf{r}$  associated with the matrix  $\mathbf{C}_{\hat{\mathbf{v}}}$  is bounded below by the corresponding form associated with the matrix  $\mathbf{I}^{-1}$

$$\mathbf{r}^T \mathbf{C}_{\hat{\mathbf{v}}} \mathbf{r} \geq \mathbf{r}^T \mathbf{I}^{-1} \mathbf{r}. \quad (4)$$

In particular, for the vector  $\mathbf{r}$  whose components are all equal to zero except for  $r_i = 1$ , the inequality 4 defines the lower bound for the variance of the parameter estimate  $\hat{v}_i$

$$\sigma^2(\hat{v}_i) = [\mathbf{C}_{\hat{\mathbf{v}}}]_{ii} \geq [\mathbf{I}^{-1}]_{ii}. \quad (5)$$

It is easy to derive  $\mathbf{I} = \mathbf{J} + \mathbf{L}$ , where

$$J_{ij} = \frac{1}{2} \frac{\partial^2 \ln |\mathbf{C}_{\mathbf{U}}|}{\partial v_i \partial v_j} + \frac{1}{2} \text{Sp} \left( \frac{\partial^2 \mathbf{C}_{\mathbf{U}}^{-1}}{\partial v_i \partial v_j} \mathbf{C}_{\mathbf{U}} \right) \quad (6)$$

and

$$L_{ij} = \left( \frac{\partial \bar{\mathbf{U}}}{\partial v_i} \right)^T \mathbf{C}_{\mathbf{U}}^{-1} \left( \frac{\partial \bar{\mathbf{U}}}{\partial v_j} \right). \quad (7)$$

The matrix  $\mathbf{L}^{-1}$  is an estimator of the covariance matrix for Least Square Fitting with linearization of the vector  $\mathbf{U}$  with respect to the parameters  $\mathbf{v}$ . Usually this approach is used for estimation of track parameters. In practice, it also provides quite good estimation for track parameter variances. Therefore one can expect that the information matrix is practically determined by  $\mathbf{I} \approx \mathbf{L}$ .

The reasons of this low significance of  $\mathbf{J}$  for an information about track parameters are the following. As usual, the configuration of trackers in a forward spectrometer is a set of detector planes being mounted in layers perpendicular to the beam axis. The derivatives of the elements of the  $\mathbf{C}_{\mathbf{U}}$  matrix with respect to  $x$  and  $y$  are equal to

zero. The dependence of  $\mathbf{C}_{\mathbf{U}}$  on the track slope appears in terms related to multiple scattering because the length  $l$  of the path through the detector plane of thickness  $h$  is  $l = h\sqrt{1 + t_x^2 + t_y^2}$ . Derivatives of  $\mathbf{C}_{\mathbf{U}}$  with respect to a track slope  $t_x$  certainly include the multipliers

$$\frac{\partial l}{\partial t_x} = \frac{h \cdot t_x}{\sqrt{1 + t_x^2 + t_y^2}}$$

proportional to the small parameter  $t_x$ . The same is true for  $t_y$ . Measurement resolutions, also contributing to elements of the matrix  $\mathbf{C}_{\mathbf{U}}$ , typically do not depend on track slopes or this dependence is very flat for small  $t_x, t_y$ . The values of the derivatives  $\partial \bar{\mathbf{U}} / \partial t_x$  defining  $\mathbf{L}$  depend on the model for the measurement  $\mathbf{U}$ . If  $U_i$  is a measurement related to the track slope  $t_x$  then the derivative  $\partial U_i / \partial t_x \approx 1$ . In the case when  $U_i$  is a measurement related to the track coordinate  $x$  then  $\partial U_i / \partial t_x \approx z_i - z_1$ . In any case, some of  $\mathbf{U}$  derivatives with respect to a track slope are significant in contrast to the derivatives of the  $\mathbf{C}_{\mathbf{U}}$  elements which are always small.

The dependence of the  $\mathbf{C}_{\mathbf{U}}$  matrix on the momentum will be discussed in more detail. For high momenta the matrix  $\mathbf{C}_{\mathbf{U}}$  is determined by the geometry and resolutions of the detector and derivatives of its element with respect to the momentum parameter  $q$  are small. For lower momenta the part of  $\mathbf{C}_{\mathbf{U}}$  influenced by multiple scattering definitely depends on  $q$ . But effects determining the “knowledge” about the momentum and influencing  $\mathbf{J}$  and  $\mathbf{L}$  are different. The effect of particle trajectory disturbance due to multiple scattering and subsequent spread of measurements with respect to a mean trajectory is taken into account in the matrix  $\mathbf{J}$ . The deflection of the particle trajectory in a magnetic field is the source of the knowledge about the momentum and it influences the matrix  $\mathbf{L}$ . We can expect that the latter effect is more important. Later, for a specified model of measurement  $\mathbf{U}$  we will show that  $L_{qq} \gg J_{qq}$ .

### 3 Spectrometer with magnet tracking

The case when tracking detectors are placed inside the magnet will be discussed first. Let us consider a process most significant for momentum resolution, an evolution of the track slope in the bending plane. The mean trajectory of a particle in a magnetic field  $\mathbf{B}$  satisfies the equation of motion:

$$\frac{d\vec{t}_x}{ds} = q \cdot c \cdot \left[ \vec{t}_y \cdot (\vec{t}_x B_x + B_z) - (1 + \vec{t}_x^2) B_y \right], \quad (8)$$

where  $c$  is a constant and  $s$  the track length. In the case of relatively small slopes we obtain the following solution for the track slope in the bending plane

$$\vec{t}_i = \vec{t}_{i-1} + \Delta t_i, \quad (9)$$

where the deflection of the slope is (we drop the subscript  $x$  on  $t$  and  $y$  on  $B$ )

$$\Delta t_i = -q c \int_{s_{i-1}}^{s_i} B ds = q \beta_i, \quad (10)$$

where  $\beta_i$  is a constant. The dependence of the dispersion due to multiple scattering is also approximately linear in  $q$

$$\delta_i = q \alpha_i, \quad (11)$$

where  $\delta_i$  is the RMS of the slope deviation with respect to the mean trajectory for the path from  $s_{i-1}$  to  $s_i$ , and  $\alpha_i$  is a constant. Definitely, for some detector planes  $|\Delta t_i| \gg \delta_i$ , otherwise a detector could not be considered as a spectrometer. For example, in the HERA-B spectrometer the ratio  $|\Delta t_i|/\delta_i$ , averaged over the fifth tracking detector located in the strong magnetic field is about of 45.

Let us assume that detectors are measuring slopes in the bending plane and multiple scattering is dominating, i.e. that we can neglect measurement errors. The slope at the beginning of the track is already defined as  $t_1 = t$  and only  $t_2, t_3, \dots, t_N$  are random variables. A charge particle traversing a medium is described by a Markov process, i.e. a random process whose future probabilities are determined by its most recent values. Therefore the probability density has the form

$$f(t_2, t_3, \dots, t_N | t_1, q) = \prod_{i=2}^N f(t_i | t_{i-1}, q). \quad (12)$$

We also consider multiple scattering as a Gaussian process. The conditional probability density  $f(t_i | t_{i-1}, q)$  is given by

$$f(t_i | t_{i-1}, q) = \frac{1}{\sqrt{2\pi}\delta_i} \exp \left[ -\frac{1}{2\delta_i^2} [(t_i - t_{i-1}) - \mathbf{E}(t_i - t_{i-1})]^2 \right], \quad (13)$$

where only deviations  $t_i$  with respect to  $t_{i-1}$  are considered as random variables. The vector

$$\mathbf{U}^T = (t_2 - t_1, t_3 - t_2, \dots, t_N - t_{N-1}).$$

has a diagonal covariance matrix

$$[\mathbf{C}_U]_{ii} = \delta_i^2 \quad (14)$$

and the vector of derivatives is

$$\left( \frac{\partial \bar{\mathbf{U}}}{\partial q} \right)^T = (\beta_2, \beta_3, \dots, \beta_N). \quad (15)$$

Using eqs. 6, 7, 10, 11, 14 and 15 it is easy to obtain

$$J_{qq} = \sum_i \frac{2}{q^2} = \frac{2(N-1)}{q^2} \quad (16)$$

and

$$L_{qq} = \sum_i \frac{\Delta t_i^2}{\delta_i^2} \frac{1}{q^2}. \quad (17)$$

It has already been mentioned, that for some planes inside the magnet  $|\Delta t_i| \gg \delta_i$  and therefore  $L_{qq} \gg J_{qq}$  in accordance with expectation. The inequality for the momentum resolution finally looks as

$$\frac{\sigma(q)}{q} \geq \left( \sum_i \frac{\Delta t_i^2}{\delta_i^2} \right)^{-\frac{1}{2}}. \quad (18)$$

According to eq. 10 the deflection  $\Delta t_i$  is proportional to  $B$  and only the terms corresponding to a significant  $B$  mainly contribute to the sum in the latter relation. Therefore only multiple scattering in the area of significant magnetic field influences the momentum resolution.

## 4 Spectrometer without track measurement inside the magnet

In this case the measurements are not inside the magnet. Let us assume that all detectors upstream of the magnet have measured the slope  $t_1$  with an error  $\sigma_1$  and downstream the slope  $t_2$  with an error  $\sigma_2$ . The mean values  $\bar{t}_1, \bar{t}_2$ , the slope deflection  $\Delta t$  and the dispersion due to multiple scattering in the magnet  $\delta$  satisfy relations similar to eqs. 9, 10 and 11, correspondingly. The vector of parameters is

$$\mathbf{v}^T = (t, q),$$

where  $t$  is a slope and  $q$  a momentum parameter at the beginning of track. The vector of measurements is

$$\mathbf{U}^T = (t_1, t_2),$$

and the covariance matrix

$$\mathbf{C}_U = \begin{pmatrix} \sigma_1^2 & 0 \\ 0 & \sigma_2^2 + \delta^2 \end{pmatrix}. \quad (19)$$

The vectors of derivatives are

$$\left( \frac{\partial \bar{\mathbf{U}}}{\partial t} \right)^T = (1, 1) \quad \text{and} \quad \left( \frac{\partial \bar{\mathbf{U}}}{\partial q} \right)^T = (0, \beta).$$

With the approximation  $\mathbf{I} \approx \mathbf{L}$  it is possible to derive

$$\mathbf{I} \approx \frac{1}{\sigma_2^2 + \delta^2} \begin{pmatrix} (\sigma_1^2 + \sigma_2^2 + \delta^2)/\sigma_1^2 & \beta \\ \beta & \beta^2 \end{pmatrix}. \quad (20)$$

With the inverse matrix

$$\mathbf{I}^{-1} = \begin{pmatrix} \sigma_1^2 & -\sigma_1^2/\beta \\ -\sigma_1^2/\beta & (\sigma_1^2 + \sigma_2^2 + \delta^2)/\beta^2 \end{pmatrix} \quad (21)$$

we find the lower bound for the dispersion of the track slope

$$\sigma(t)^2 \geq [\mathbf{I}^{-1}]_{11} = \sigma_1^2 \quad (22)$$

and of the inverse momentum

$$\sigma(q)^2 \geq [\mathbf{I}^{-1}]_{qq} = \frac{\sigma_1^2 + \sigma_2^2 + \delta^2}{\beta^2}. \quad (23)$$

In the approximation considered here, the information from the slope measurement after the magnet ( $t_2$ ) does not contribute to the angular resolution in (22) and is influencing only the momentum resolution

$$\frac{\sigma(q)}{q} \geq \frac{(\sigma_1^2 + \sigma_2^2 + \delta^2)^{\frac{1}{2}}}{\Delta t}. \quad (24)$$

The dispersion ( $\delta$ ) in the latter relation takes into account multiple scattering in the whole material on the path from last point on track segment in front of magnet up to first point of segment behind the magnet. From the latter relation is clear that by improving angular resolutions of tracking detectors in front of the magnet and behind it ( $\sigma_1, \sigma_2$ ) and minimizing multiple scattering inside the magnet ( $\delta$ ) we can achieve high momentum resolution even without track measurements inside the magnet.

## 5 Momentum reconstruction in the HERA-B spectrometer

The tracking detectors of the HERA-B forward spectrometer [1] consist of the vertex detector system (VDS) for precision measurement of vertices and the main tracker dedicated to momentum measurement and triggering. The detector planes are mounted in layers perpendicular to the beam axis. The silicon microstrip detectors are used in the VDS placed in front of the magnet. The inner tracker (ITR) uses microstrip gas chamber (MSGC) detectors for the inner part of the main tracker up to distances 25 cm from the beam. The outer tracker (OTR) uses honeycomb drift chambers to fill the remaining acceptance with in total 1000 m<sup>2</sup> of active area.

The main tracker contains tracking devices inside and behind the magnet. The part of the main tracker behind the magnet is called the pattern chamber area (PC). The RICH detector is located behind the PC. Two additional tracker superlayers behind the RICH are mainly used by the first level trigger. This trigger chamber area (TC) also serves together with the PC to provide additional measurement of the track position and slopes. The typical size of the magnetic field components ( $B_x, B_y, B_z$ ) are shown in fig. 1 as functions of  $z$  and  $x$ . The main bending component ( $B_y$ ) is significantly inhomogeneous, with a bell-shaped dependence on  $z$ , varying with  $x$ .

To improve the conditions for the detection of electrons, for the year 2002 data taking the OTR/ITR detectors inside the magnet were removed, except for one OTR/ITR superlayer located in front of the magnet in a low magnetic field. This geometry of the OTR/ITR will be discussed in the following.

The angular and momentum resolution has been evaluated with single muons generated with HBGEAN [3], the GEANT based simulation program for the HERA-B detector. The multiple scattering was simulated according to the Molière theory.

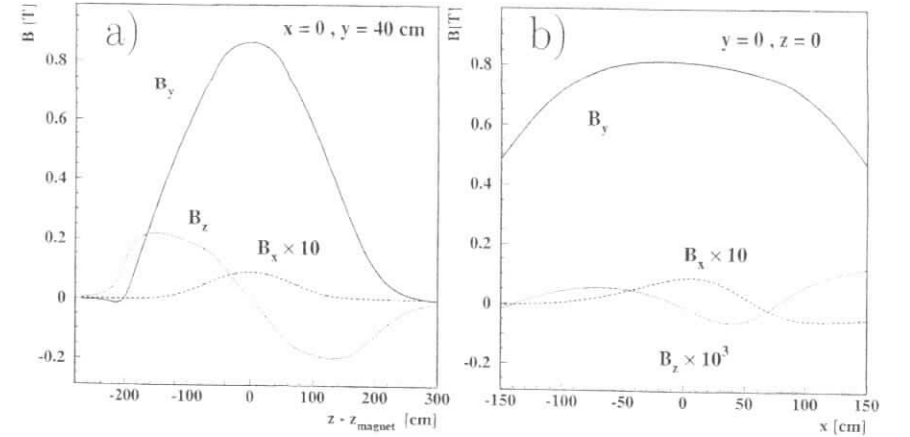


Figure 1: Field components of the HERA-B magnet as function of the coordinates. The axis  $x$  belongs to the main bending plane of the magnet and is perpendicular to the beam. Coordinates are given relative to the magnet center. a) Magnetic field components as a function of the  $z$  coordinate at a vertical displacement of 40 cm. b) Magnetic field components as a function of the  $x$  coordinate.

Continuous energy loss with generation of  $\delta$ -rays above a certain cut energy and Landau fluctuations below this energy were used for simulation of charged particles traversing a medium. The simulated muons had a fixed momentum and a uniform pseudorapidity distribution ( $2.5 \leq \eta \leq 4.5$ ). For the simulation of hits in the detectors, the following hit resolutions have been used: 12  $\mu\text{m}$  for the VDS, 400  $\mu\text{m}$  for the OTR and 150  $\mu\text{m}$  for the ITR.

The standard reconstruction procedure for the HERA-B tracker was used. The track segments were reconstructed independently in the VDS and the PC area. Track segments from the PC area were prolonged into the TC area [4]. The VDS and PC segments were matched to form VDS-PC-TC tracks. The hits belonging to a track were fitted [5]. For the propagation of the track parameters through the magnetic field the approach described in [6] was used.

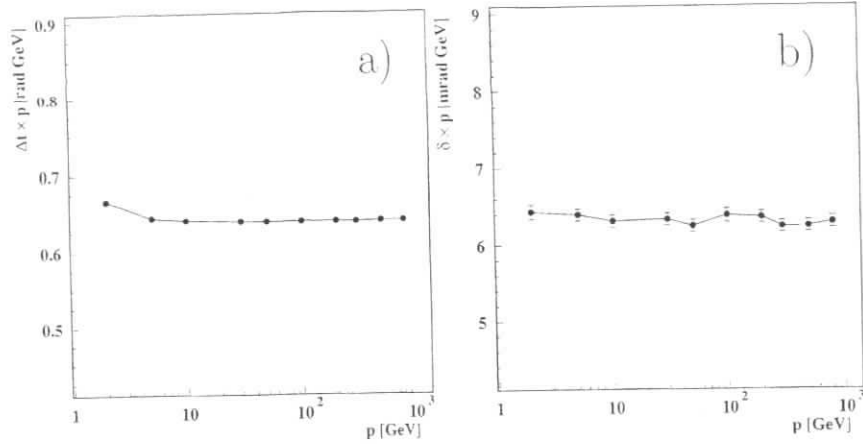


Figure 2: Particle parameters multiplied by the momentum  $p$  as a function of  $p$ . a) Deflection of the track slope in the magnet ( $\Delta t$ ). b) The RMS of the slope fluctuation due to multiple scattering in the magnet ( $\delta$ ).

## 6 The relation between angular and momentum resolutions

The considered geometry of the OTR/ITR detectors corresponds to the configuration of a forward spectrometer without track measurements inside the magnetic field. The deflection angle ( $\Delta t$ ) and the slope deviation due to multiple scattering in the magnet ( $\delta$ ) are approximately in agreement with eqs. 10 and 11. This is seen in fig. 2 where corresponding parameters are displayed for the values of muon momenta from 2 GeV up to 800 GeV. The products ( $\Delta t \cdot p$ ) and ( $\delta \cdot p$ ) are approximately constant despite the significantly inhomogeneous magnetic field and the rather complicated structure of the main tracker. Therefore we can expect that relations derived for resolutions will also be approximately valid.

With the PC segments, by a stand-alone reconstruction in the area behind the magnet it is possible to make a crude momentum estimation based on the average momentum “kick” in the magnetic field according to eq. 10. This momentum estimation is important for the calculation of covariance matrices used in the stand-alone segment fitting. For the VDS segments in front of the magnet such momentum estimation is not possible. Therefore we refitted the VDS segments after the calculation of the covariance matrices based on momentum estimation for the corresponding PC segments matched with them. The slope  $t_x$  of these refitted VDS segments we compared with the slope for corresponding VDS-PC-TC tracks. These slope resolutions shown in fig. 3 are similar for all considered

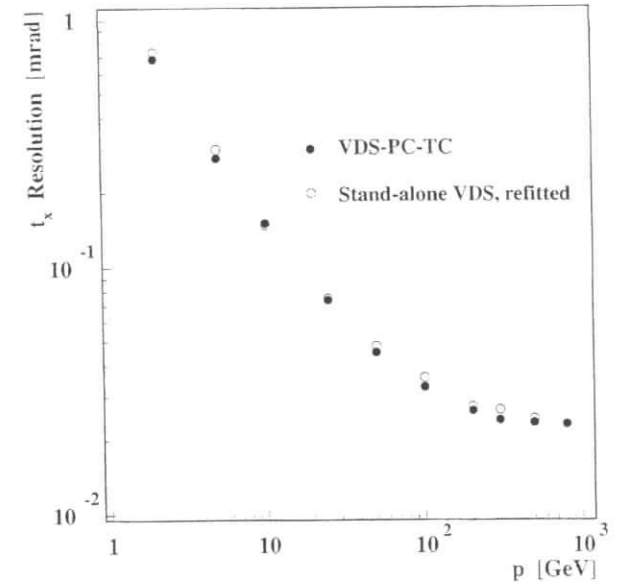


Figure 3: Resolution of the slope parameter  $t_x$  as a function of momentum  $p$  for VDS-PC-TC tracks (filled circles) and VDS segments in front of the magnet (open circles) refitted with the covariance matrices based on the momentum estimation from the matched PC segments.

momenta. This is in agreement with expectation from eq. 22.

Inequality 24 predicts contributions of different factors to the momentum resolution. These factors are: the slope resolutions of track segments in front and behind the magnet, and multiple scattering in the material inside the magnet. The values of these parameters as a function of momentum are shown in fig. 4. The quadratic sum of these three contributions divided by the slope deflection in the magnet gives us a guess of the momentum resolution. This crude estimation is compared in fig. 5 with values of momentum resolution evaluated for fully reconstructed and fitted VDS-PC-TC tracks. The values are in agreement with the expectations from eq. (24).

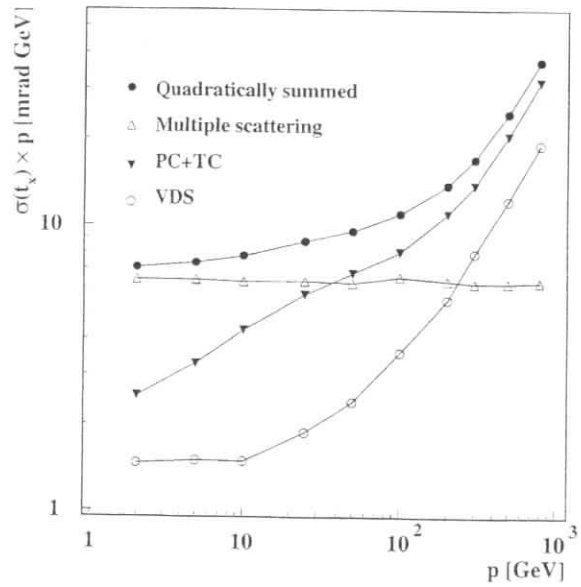


Figure 4: Slope resolution  $\sigma(t_x)$  multiplied by the momentum  $p$  for VDS segments in front of the magnet (open circles), for PC-TC segments behind the magnet (filled triangles) and the RMS of the slope deviation due to multiple scattering in the magnet ( $\delta$ ) multiplied by  $p$  (open triangles). These three values are quadratically summed (filled circles).

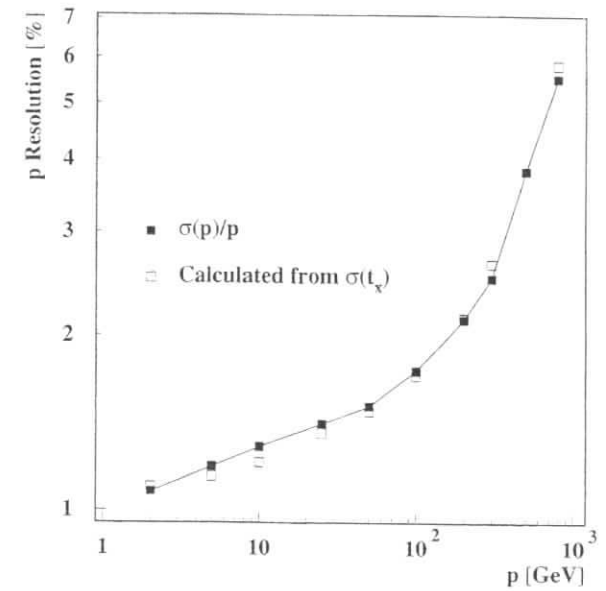


Figure 5: Momentum resolution as a function of momentum  $p$ . Crude estimation according to eq. 24 (open squares) and the value  $\sigma(P)/p$  defined for the fully reconstructed and fitted VDS-PC-TC tracks (filled squares). The value  $\sigma(P)$  is the result of a Gaussian fit of the distribution of reconstructed momentum residuals with respect to the Monte Carlo truth.

## 7 Summary

The contribution of multiple scattering to momentum resolution in the forward spectrometer depends on the configuration of the tracking system before, behind and inside the magnet. Reasons to place tracking detectors inside the magnet are usually to increase detector acceptance or pattern recognition capabilities rather than to improve the momentum resolution. In the case when the tracking detectors inside the magnet also are used for momentum reconstruction, only multiple scattering in the area with a significant magnetic field contributes to the momentum resolution.

Without track measurements in the magnetic field, multiple scattering in the whole material on the path from the last point on the track segment in front of magnet up to first point of segment behind the magnet contributes to the momentum resolution. Improving angular resolutions of tracking detectors in front of the magnet and behind it and minimizing multiple scattering inside the magnet, we can achieve high momentum resolution even without magnet tracking.

Single muons were simulated for the HERA-B spectrometer. The momentum resolution of fully reconstructed and fitted tracks is in agreement with the simple relation between the angular resolution of track segments in front and behind the magnet and estimation of multiple scattering in the material inside the magnet.

**Acknowledgments:** I would like to thank G. Böhm, H. Kolanoski and T. Lohse for the careful reading of the manuscript and discussion. I am grateful to DESY Zeuthen for the kind hospitality extended to me during my visit.

## References

- [1] T. Lohse et al. (HERA-B Collaboration), DESY-PRC 94/02 (1994).
- [2] C.R. Rao, *Linear statistical inference and its applications*. J.Wiley, New York, 1965.
- [3] S. Nowak, *HBGEAN. A description of HERA-B GEANT*, HERA-B note 94-123 (1994).
- [4] R. Mankel, *A Concurrent Track Evolution Algorithm for Pattern Recognition in the HERA-B Main Tracking System*, Nucl. Instr. Methods, **A395** (1997) 169;  
R. Mankel and A. Spiridonov, *Ranger – a Pattern Recognition Algorithm for the HERA-B Main Tracker System. Part III: Tracking in Trigger Chambers*, HERA-B note 98-206 (1998);  
A. Spiridonov, *Track Reconstruction in the High Rate Environment of the HERA-B Spectrometer*, in Proceedings of CHEP2001, Sept. 2001, Beijing, P.R. China. Science Press Beijing New York (2001) p.168.
- [5] R. Mankel, *Ranger – a Pattern Recognition Algorithm for the HERA-B Main Tracker System. Part IV: The Object-Oriented Track Fit*, HERA-B note 98-079 (1998).

- [6] A. Spiridonov, *Optimized Integration of the Equation of Motion of a Particle in the HERA-B Magnet*, HERA-B Note 98-133 (1998).

